Published in final edited form as:
J Neurosci Res. 2011 December ; 89(12): 1997–2007. doi:10.1002/jnr.22606.

Brain [U-^{13}C]glucose Metabolism in Mice with Decreased α-Ketoglutarate Dehydrogenase Complex Activity

Linn Hege Nilsen[1], **Qingli Shi**[2], **Gary E. Gibson**[2], and **Ursula Sonnewald**[1]

[1]Department of Neuroscience, Faculty of Medicine, Norwegian University of Science and Technology (NTNU), Trondheim, Norway

[2]Weill Cornell Medical College/Burke Medical Research Institute, White Plains, New York, USA

Abstract

The activity of the α-ketoglutarate dehydrogenase complex (KGDHC), a mitochondrial enzyme complex which mediates the oxidative decarboxylation of α-ketoglutarate in the TCA cycle, is reduced in Alzheimer's Disease. We investigated the metabolic effects of a partial KGDHC activity reduction on brain glucose metabolism using mice with disrupted expression of dihydrolipoyl succinyltransferase (DLST; gene encoding the E2k subunit of KGDHC). Brain tissue extracts from cortex and cerebellum of 6-week –old heterozygote DLST knockout mice (DLST+/−) and corresponding wild type mice injected with [U-^{13}C]glucose and decapitated 15 minutes later were analyzed. An increase in the concentration of glucose in cortex suggested a decrease in the cortical utilization of glucose in DLST +/− mice. Furthermore, the concentration and ^{13}C labelling of aspartate in cortex were reduced in DLST+/− mice. This decline was likely caused by a decrease in the pool of oxaloacetate. In contrast to results from cell culture studies, no indications of altered glycolysis or GABA shunt activity were found. Glucose metabolism in the cerebellum was unaffected by the decrease in KGDHC activity. Among metabolites not related to glucose metabolism, the concentration of taurine was decreased in the cortex, and that of tyrosine was increased in the cerebellum. These results imply that diminished KGDHC activity has the potential to induce the reduction in glucose utilization that is seen in several neurodegenerative diseases.

Keywords

glucose; glutamate; Alzheimer's Disease; magnetic resonance spectroscopy

Introduction

Normal brain function depends upon oxidation of glucose, in which glycolysis and the tricarboxylic acid (TCA) cycle play crucial roles. The α-ketoglutarate dehydrogenase complex (KGDHC; EC 1.2.4.2, EC 2.3.1.61, EC 1.8.1.4) is a key enzyme in the TCA cycle, in which it mediates the oxidative decarboxylation of α-ketoglutarate (α-KG) to succinyl coenzyme A. α-KG is also a precursor for the synthesis of glutamate in neurons and astrocytes, which can be further converted to GABA in GABAergic neurons and to glutamine in astrocytes. It can be hypothesized that even moderate reduction in KGDHC activity has the potential to affect mitochondrial metabolism and amino acid neurotransmitter homeostasis in the brain. Indeed, diminished KGDHC activity has been

Corresponding author: Dr. U. Sonnewald, Dept. Neuroscience, Faculty of Medicine, Olav Kyrresgt. 3, N-7489 Trondheim, Norway, Tel. +47-73 590492; FAX +47-73 598655, ursula.sonnewald@ntnu.no.

linked to a variety of neurodegenerative diseases in which mitochondrial dysfunction occurs [for a review see (Gibson et al. 2000b)], and mounting evidence implicates decreased KGDHC activity in Alzheimer's Disease (AD). Post mortem measurements of enzyme activity in AD brain tissue reveal reductions ranging from 25 % to 75 % (Bubber et al. 2005; Butterworth and Besnard 1990; Gibson et al. 2000a; Gibson et al. 1988; Mastrogiacomo et al. 1993), and the activity of the enzyme complex is reduced in both pathologically affected and unaffected brain areas (Gibson et al. 1988). Moreover, the decrease in KGDHC activity correlates with the degree of cognitive impairment in patients with AD (Bubber et al. 2005). Reduced glucose metabolism in the brain is one of the most common characteristics of AD, and can precede clinical symptoms by decades (Mosconi et al. 2008; Reiman et al. 1996; Small et al. 1995). The relation between decreased KGDHC activity and hypometabolism is, however, not clear. It is possible that diminished KGDHC activity might contribute to or cause the decreased glucose metabolism in AD. Because numerous mechanisms may alter KGDHC activity *in vivo*, more knowledge about the consequences of reduced KGDHC activity is necessary and may shed light on possible pathophysiological mechanisms in AD and other neurodegenerative diseases.

KGDHC consists of three different proteins; E1k (α-KG dehydrogenase; KGDH), E2k (dihydrolipoyl succinyltransferase; DLST) and E3 (dihydrolipoyl dehydrogenase; DLD), and E1k and E2k are specific for KGDHC. To address the question of how a partial reduction of KGDHC activityaffects glucose metabolism in the brain, we investigated this in the cerebral cortex and cerebellum of mice with reduced KGDHC activity as a consequence of partial genetic deletion of the E2k subunit. Previously performed measurements in whole brain homogenates of 6-week-old DLST +/− mice showed about 50 % reduction of DLST mRNA and protein, whereas mRNA and protein of the other subunits remained unaltered (Yang et al. 2009). KGDHC activity was not measured in the current study, but has previously been examined in mice with the DLST +/− genotype using two different methods; an enzymatic assay measuring α-KG dependent conversion of NAD^+ to NADH showing a ~ 40 % reduction in whole-brain homogenates, and *in situ* histochemistry activity staining showing a 79 % reduction in cortex and a 86 % reduction in cerebellum (Yang et al. 2009). No bioenergetic abnormalities except decreased KGDHC activity have been found in these mice, and a 50 % reduction in activity does not appear to affect development. This may be because KGDHC increases after birth and does not reach adult levels until 30 days (Buerstatte et al. 2000; Yang et al. 2009). In addition, DLST +/− mice have normal brain morphology, with no evident neurodegenerative changes or astrogliosis (Calingasan et al. 2008). In the current study, DLST +/− and wildtype mice were injected with [U-^{13}C]glucose, and metabolite concentrations and ^{13}C labelling patterns were mapped using ^{1}H and ^{13}C nuclear magnetic resonance spectroscopy, gas chromatography - mass spectrometry, high performance liquid chromatography and a glucose assay. This is the first study to examine brain metabolism in DLST +/− mice.

Materials and methods

[U-^{13}C]glucose, hexokinase (EC 2.7.1.1, Baker's yeast, S. Cerevisiae), glucose-6-phosphate dehydrogenase (EC 1.1.1.49, Baker's yeast, S. Cerevisiae), ATP and NADP were obtained from Sigma-Aldrich (St. Louis, MO, USA). Ethylene glycol was bought from Merck (Darmstadt, Germany), L-2-Aminobutyric acid (α-ABA) from Fluka (Buchs, Switzerland) and (*N*-Methyl-*N*-(*tert*-Butyldimethylsilyl)triflouroacetamide (MTBSTFA) containing 1% *tert*-Butyldimethylchlorosilane (*t*-BDMS-Cl) was obtained from Regis Technologies Inc. (Morton Grove, IL, USA). All other chemicals used were of the purest grade available from commercial sources.

Animal treatments

Sixteen mice that were hybrids of C57BL/6 and 129SV/EV with an average weight of 23.2 grams were included in the experiment. Genotyping was done as in previous experiments (Yang et al. 2009). All animals were housed in constant temperature (22 ± 8 °C), humidity (50 ± 5 %) and illumination (12 hour light; 12 hour dark) with free access to food and water. The animal experiments were approved by Weill Cornell Medical College Institutional Animal Care and Use Committee.

The control group consisted of 9 mice with the wildtype (WT) genotype (DLST +/+), and 7 mice constituted the DLST +/− group. All animals were injected intraperitoneally with 0.3 M [U-^{13}C]glucose (1 ml per 100 g) at 6 weeks of age. The mice were decapitated 15 minutes after the injection, and the heads were snap frozen in liquid nitrogen and stored at −80 °C. Blood was collected from the bodies, quickly pipetted into tubes and centrifuged at 800 g for 5 minutes. Serum was separated and stored at −80 °C. Cerebral cortex and cerebellum were dissected on ice, weighed and stored at −80 °C till extraction.

Tissue and serum extraction

Frozen cortex samples were homogenized in a 2.4 ml solution consisting of ethanol (70 %) and 250 μM α-ABA using a Vibra Cell sonicator (Model VCX 750, Sonics & Materials, Newtown, CT, USA), centrifuged at 3000 g and 4 °C for 5 minutes, and the supernatants were transferred to new tubes. The precipitates were re-dissolved in 500 μl ethanol (70 %) and centrifuged again, and the supernatants were pooled. Cerebellum samples were homogenized in a 2 ml solution of perchloric adic (PCA, 7%) and 250 μM α-ABA. Except for the following steps, the extraction of cerebellar tissue was similar to that for the cortex: 20 μl were taken out for HPLC analysis from the first supernatant, and the precipitates were re-dissolved in 500 μl PCA (7%) instead of ethanol. pH of the cerebellum supernatants was adjusted to 6.5–7.5 with KOH (1 M) and $KClO_4$ was removed with centrifugation. The samples were kept on ice whenever possible during the extraction procedure. All supernatants were frozen at −80 °C, lyophilized and stored at −20 °C.

Serum samples were dissolved in 200 μl PCA (7%) and centrifuged at 9800 g at 4 °C for 15 minutes. The supernatants were transferred to new tubes and pH was adjusted to 6.5–7.5 with KOH (1 M). $KClO_4$ was removed with centrifugation. The supernatants were then lyophilized. The resulting powders were re-dissolved in 200 μl D_2O (99%), centrifuged at 1600 g for 10 minutes and supernatants were transferred to new tubes. These were then frozen, lyophilized, re-dissolved in D_2O again, centrifuged and supernatants were transferred to new tubes before another lyophilization. The samples were then stored at −20 °C.

High performance liquid chromatography (HPLC)

High performance liquid chromatography HPLC) (1100 series, Agilent Technologies Inc., Santa Clara, CA, USA) with fluorescence detection was utilized to quantify metabolite concentrations in cerebellum. Amino acids were pre-column derivatized with *o*-phthaldialdehyde. Components were separated on a ZORBAX SB-C18 column (4.6 × 150 mm, 3.5 micron particle diameter, Agilent Technologies) using a gradient of two eluents to achieve optimal separation and faster elution of the most non-polar analytes. One eluent consisted of phosphate buffer (50 mM, pH = 5.9) and tetrahydrofuran (THF) (2.5 %) and the other of methanol (98.75 %) and THF (1.25 %). Quantification was achieved by comparison with an external standard curve derived from a series of standard solutions of amino acids run before the samples. Standards were also run after every fourth sample as controls. Concentrations were corrected for potential metabolite loss during extraction using α-ABA

as an internal standard. All concentrations were also corrected for tissue weight to account for any potential variation in the size of the dissected brain areas.

Glucose assay

An aliquot of the cortex and cerebellum samples was assayed for glucose content in a coupled enzymatic assay by measuring the increase of NADPH formed in the conversion of glucose-6-phosphate to 6-phosphogluconolactone, essentially as described previously (Bergmeyer et al. 1974). Lyophilized samples were reconstituted in 5 mM potassium acetate buffer (pH 4.5) and an aliquot was transferred to a microtiter plate. Subsequently, $MgCl_2$ (12.1 mM), ATP (0.81 mM) and NADP (0.16 mM) was added in an alkaline solution (100 mM HEPES, pH 7.5) to ensure pH-optimum (7–8) for hexokinase and glucose-6-phosphate dehydrogenase. The reaction was initiated by the addition of glucose-6-phosphate dehydrogenase (0.54 U/ml) and hexokinase (1.52 U/ml) in a HEPES buffer (100 mM HEPES, 0.0006% bovine serum albumin, pH 7.5). Following 1½ hours of incubation at 37 °C, the NADPH content was measured fluorometrically using 360 nm as excitation wavelength and 415 nm as emission wavelength. Glucose (concentration range: 12.5–500 μM) was used as standard.

^{1}H and ^{13}C nuclear magnetic resonance spectroscopy

The amounts of positional isotopomers from metabolism of [U-^{13}C]glucose and total amounts of metabolites in cortex were quantified with ^{13}C and ^{1}H nuclear magnetic resonance (NMR) spectroscopy, respectively. Lyophilized samples were dissolved in 200 μl 99% D_2O containing 0.1% ethylene glycol as an internal standard. pH was adjusted to 6.5–7.5, and the samples were transferred to 5 mm Shigemi NMR microtubes (Shigemi Inc., Allison Park, PA, USA). Spectra were obtained using a BRUKER DRX500 spectrometer (BRUKER Analytic GmbH, Rheinstetten, Germany). ^{1}H NMR spectra were acquired with the following parameters: a pulse angle of 90°, acquisition time of 2.04 seconds and a relaxation delay of 10 seconds. The number of scans was typically 320. A low-power presaturation pulse was applied at the water frequency to achieve water suppression. Proton decoupled ^{13}C NMR spectra were acquired with the following parameters: pulse angle of 30°, acquisition time of 1.3 seconds and a relaxation delay of 0.5 seconds. The number of scans was typically 42 000. Part of a typical ^{13}C NMR spectrum from a DLST +/− mouse is shown in figure 1.

Relevant peaks in the NMR spectra were identified and integrated using XWINNMR software (BRUKER BioSpin GmbH, Rheinstetten, Germany). Amounts of ^{13}C labelled positional isotopomers were quantified from the integrals of the peak areas in the ^{13}C spectra using ethylene glycol as an internal standard. Correction for nuclear Overhauser and relaxation effects was applied to all resonances, and monolabelled isotopomers were corrected for natural abundance of ^{13}C. Total amounts of metabolites were quantified from integrals of the peak areas in the ^{1}H spectra using ethylene glycol as an internal standard, and corrected for the number of protons constituting the signal of the peak. All concentrations determined with NMR spectroscopy were corrected for tissue weight to account for any potential variation in the size of the dissected brain areas.

Lyophilized serum samples were re-dissolved in 200 μl D_2O containing 0.1% ethylene glycol, and pH was adjusted to 6.5–7.5. Following centrifugation at 1600 g for 10 minutes, samples were transferred to Shigemi tubes. ^{1}H NMR spectra without water suppression (in order to quantify glucose in serum) were acquired on the same spectrometer with the following parameters: a pulse angle of 90°, acquisition time of 1.64 seconds and a relaxation delay of 10 seconds. The number of scans was typically 320.

Gas chromatography – mass spectrometry

The distribution of ^{13}C labelled mass isotopomers for several metabolites in both cortical and cerebellar samples was determined using gas chromatography-mass spectrometry (GC-MS). Because of the small size of cerebellum and thus sensitivity issues with NMR spectroscopy, information on ^{13}C labelling of metabolites in cerebellum was obtained with GC-MS only. Aliquots of the samples were dissolved and adjusted to pH < 2 using HCl, followed by lyophilization. Amino acids and organic acids were extracted into an organic phase of ethanol and benzene, dried under air again and re-dissolved in N,N-Dimethylformamide before derivatization with MTBSTFA in the presence of 1% t-BDMS-Cl. All samples were analyzed using an Agilent 6890N gas chromatograph linked to an Agilent 5975 B mass spectrometer with an electron ionization source (both from Agilent Technologies). The results were corrected for natural abundance of ^{13}C using standard solutions that were run before the samples.

^{13} C labelling patterns originating from metabolism of [U-^{13}C]glucose

Metabolism of [U-^{13}C]glucose yields specific ^{13}C labelled metabolite isotopomers depending on the metabolic pathways that were active in the time window in which ^{13}C was incorporated. Detection of the resulting ^{13}C labelling patterns with ^{13}C NMR spectroscopy and MS thus allows for detailed metabolic mapping of how cells use glucose. The following description is a simplification of possible labelling patterns originating from metabolism of [U-^{13}C]glucose. An overview is also illustrated in figure 2.

Glucose is taken up into neurons and astrocytes in equal amounts (Nehlig et al. 2004), but more ^{13}C labelled acetyl Coenzyme A (acetyl CoA) derived from glucose is metabolized in the neuronal TCA cycle (Hassel et al. 1995; Qu et al. 2000). Glycolytic metabolism of [U-^{13}C]glucose gives rise to [U-^{13}C]pyruvate, which can be converted to [U-^{13}C]lactate or [U-^{13}C]alanine. Pyruvate can also be converted to [U-^{13}C]acetyl CoA via the pyruvate dehydrogenase complex (PDHC; EC 1.2.4.1, EC 2.3.1.12, EC 1.8.1.4), enters the TCA cycle, and after several steps give rise to [4,5-^{13}C]α-KG. The latter can be further metabolized and give rise to [1,2-^{13}C]- or [3,4-^{13}C]oxaloacetate (OAA) after several steps in the first turn of the TCA cycle (two isotopomers are formed because of scrambling of the ^{13}C label in the symmetrical molecule succinate). Labelled OAA can be transaminated to [1,2-^{13}C]- or [3,4-^{13}C]aspartate, or it can condense with labelled or unlabelled acetyl CoA and give rise to different labelling patterns in later turns of the TCA cycle [(for more detailed labelling patterns see (Bak et al. 2006)]. Alternatively, [4,5-^{13}C]α-KG can leave the TCA cycle by being converted to [4,5-^{13}C]glutamate. In astrocytes, [4,5-^{13}C]glutamate is further converted to [4,5-^{13}C]glutamine via the enzyme glutamine synthetase (GS; EC 6.1.3.2) (Norenberg 1979; Norenberg and Martinez-Hernandez 1979). Glutamate can be released from neurons during neurotransmission, and astrocytes terminate the signal by taking up glutamate and converting it to α-KG or to [4,5-^{13}C]glutamine. Inhibiting the astrocytic TCA cycle with fluoroacetate has shown that approximately 40% of the glutamine labelled from the first turn of the TCA cycle originates from glutamate labelled in the neuronal compartment (Hassel et al. 1997). In GABAergic neurons, [4,5-^{13}C]glutamate can be decarboxylated to [1,2-^{13}C]GABA via the enzyme glutamic acid decarboxylase (GAD; EC 4.1.1.15) (Roberts and Frankel 1950; Saito et al. 1974) and released to the synapse in vesicles. GABA is removed from the synapse both via presynaptic neurons and surrounding astrocytes. In neurons, GABA can be repacked in vesicles. Alternatively, GABA is degraded through the GABA shunt, operating in both neurons and astrocytes to allow the carbon skeleton of GABA to re-enter the TCA cycle as succinate. Moreover, [4,5-^{13}C]glutamine from astrocytes can be transferred to neurons and be converted to [4,5-^{13}C]glutamate (and to [1,2-^{13}C]GABA in GABAergic neurons). Glutamate, glutamine, GABA, aspartate and TCA cycle intermediates labelled from the first turn of the TCA cycle are detected as double

labelled metabolites (M+2) with GC-MS. It should be noted, however, that M+2 isotopomers can arise from later turns of the TCA cycle as well.

Calculation of Pyruvate Carboxylase versus Pyruvate Dehydrogenase Complex activity

Pyruvate can either be converted by PDHC, or it can contribute to anaplerosis via the enzyme pyruvate carboxylase (PC; EC 6.4.1.1) in astrocytes (Shank et al. 1985; Waagepetersen et al. 2001). The contribution from the anaplerotic versus the oxidative (PDHC) pathway in the formation of glutamate, glutamine and GABA can be expressed as a ratio of isotopomers derived from PC activity over isotopomers derived from PDHC activity (Taylor et al. 1996). This was calculated as ([2,3-^{13}C] – [1,2,3-^{13}C]/[4,5-^{13}C]) for glutamate and glutamine [adapted from (Haberg et al. 1998)]. [2,3-^{13}C]glutamate or glutamine can be formed both after pyruvate carboxylation and after oxidation of [U-^{13}C]glucose via PDHC when the ^{13}C label stays in the TCA cycle until the third turn. However, when [2,3-^{13}C]glutamate or glutamine arises from the latter, an equal amount of [1,2,3-^{13}C]glutamate or glutamine will be formed. Therefore, [2,3-^{13}C]glutamate or glutamine in excess of [1,2,3-^{13}C] will represent labelling derived from pyruvate carboxylation. The corresponding ratio for GABA may be expressed as [3,4-^{13}C]/[1,2-^{13}C]GABA. Both these isotopomers are also derived from the third TCA cycle turn when the ^{13}C label entered via PDHC, but this could not be corrected for in the ratio.

Representation of ^{13}C enrichment of the acetyl CoA pool

An estimate of the contribution of a ^{13}C labelled precursor to labelling of the acetyl CoA pool is typically measured by analysis of the ^{13}C labelling of glutamate isotopomers (Jones et al. 1997). This was calculated as [3,4,5-^{13}C]glutamate/[3-^{13}C]glutamate, in other words the ratio of double/mono-labelled glutamate C-3 which represents the ^{13}C-enrichment of the acetyl-CoA pool entering the TCA cycle [adapted from (Navarro et al. 2008)], because [3,4,5-^{13}C]glutamate is formed when labelled OAA from the first turn of the TCA cycle condenses with ^{13}C labelled acetyl CoA while [3-^{13}C]glutamate is formed when OAA condenses with unlabelled acetyl CoA.

Statistical analysis

One of the mice in the DLST +/− group received a faulty injection of ^{13}C labelled glucose, apparent by lack of ^{13}C labelling as detected with both ^{13}C NMR spectroscopy and GC-MS. As a consequence of this, all ^{13}C data obtained from this mouse were excluded. The glucose assay was performed on seven WT and five DLST +/− samples for cortex because equipment failure led to a loss of volume in some samples, and nine WT and seven DLST +/− samples for cerebellum. When the percentage [U-^{13}C]glucose was calculated, the combination of the lack of measurement of total glucose for some samples and the lack of adequate ^{13}C glucose measurement for one sample led to calculation of ^{13}C enrichment of glucose in seven WT and four DLST +/− cortex samples. Four randomly chosen serum samples from each group were analyzed with ^{1}H NMR spectroscopy.

All data are presented as mean ± standard deviation. The statistical differences between WT and DLST +/− mice were assessed with the unpaired two tailed Student's *t*-test where $p < 0.05$ was considered as indicating a significant difference between the groups.

Results

Serum

The concentration of glucose and the percentage [U-^{13}C]glucose in the serum are presented in Table I. Neither were altered in DLST +/− mice.

Concentration of metabolites related to glycolysis

The concentrations of glucose, lactate and alanine are presented in Table I. The glucose concentration in cortex was significantly increased by 84 % in DLST +/− mice, whereas the concentration in cerebellum was unaltered. The glucose concentration in cortex was somewhat low, but similar concentrations have previously been reported for cortex after decapitation (Melø et al. 2007). Moreover, glucose levels in cerebellum are often higher than in cortex (Melo et al. 2005; Melø et al. 2007). The lactate concentration in cortex remained unaltered and was not measured in cerebellum. The amount of alanine was measured in both brain areas but did not change.

^{13}C labelling of metabolites related to glycolysis

A summary of the ^{13}C labelling results for glucose, lactate and alanine can be found in Table I. The percentage [U-^{13}C]glucose could only be obtained from the cortical samples, because cerebellar samples were not analyzed with ^{13}C NMR spectroscopy. The percentage ^{13}C labelled glucose in cortex was similar when comparing WT and DLST +/− mice, as both the amount of ^{13}C glucose (69.97 ± 29.60 nmol/g in WT mice and 133.51 ± 49.28 nmol/g in DLST +/− mice, $p = 0.014$) and the glucose concentration were increased in DLST +/− mice. The percentage of [U-^{13}C]lactate also remained unaltered between the groups in both cortex and cerebellum, and the percentage of [U-^{13}C]alanine was unchanged in the cortex.

Concentration of metabolites related tothe TCA cycle

The concentrations of various TCA cycle intermediates and derivatives are presented in Table II. The amounts of glutamate, glutamine and GABA were unaffected in both cortex and cerebellum. Aspartate was significantly decreased in the cortex of DLST +/− mice (29 % decreased), but remained unaltered in cerebellum. No changes were found in the concentrations of succinate and fumarate in cortex.

^{13}C labelling of metabolites related to the TCA cycle

The amounts of ^{13}C labelled positional isotopomers of glutamate, glutamine, GABA and aspartate derived from the first turn of the TCA cycle in cortex are presented in Figure 3. No significant differences between WT and DLST +/− mice were found in the amounts of [4,5-^{13}C]glutamate or [4,5-^{13}C]glutamine, or [1,2-^{13}C]GABA. However, DLST +/− mice had significantly lower amounts of both [1,2-^{13}C]- and [3-4-^{13}C]aspartate in the cortex, with reductions of ~ 25 % and 29 %, respectively. No other significant differences were found in amounts of positional isotopomers derived from TCA cycle metabolism of [U-^{13}C]glucose in cortex.

Results from GC-MS analysis show the percentage that ^{13}C mass isotopomers constitute of the total amount of the metabolite, in contrast to the ^{13}C labelling of positional isotopomers given by ^{13}C NMR spectroscopy. The percentage of metabolites with ^{13}C label in two carbon atoms of the molecules (M+2 isotopomers) in both cerebellum and cerebral cortex of both genotypes are presented in Table III. No differences were found between the groups in the percentage of any mass isotopomers (M+1, M+2, M+3) of glutamate, glutamine, GABA, aspartate, succinate, fumarate or malate (only M+2 isotopomers are presented in Table III), in line with results from NMR spectroscopy. Becausee both the total concentration of aspartate and the amount of [1,2-^{13}C] and [3,4-^{13}C]aspartate were decreased similarly in cortex, M+2 aspartate remained unchanged.

Concentrations of other metabolites

The concentration of tyrosine was increased in the cerebellum of DLST +/− mice (Table II). Tyrosine is not easily quantifiable with ^{1}H NMR spectroscopy, and was not possible to quantify in cortex. Furthermore, DLST +/− mice had a significant decrease in the amount of taurine in cortex (Table II), but no change in the concentration of N-acetyl aspartate (NAA). Several other metabolite concentrations were measured, but remained unaltered (results not shown). In cortex, these were myo-inositol, creatine, and choline. In cerebellum, these were glutathione, serine, glycine, threonine, arginine, lysine, methionine, tryptophan, valine, phenylalanine, isoleucine and leucine.

Metabolic ratios

No differences were found between the WT and DLST +/− mice when the ^{13}C enrichment of the acetyl CoA pool and the ratio PC over PDHC activity and were calculated, as shown in Table IV.

Discussion

Glucose metabolism in DLST +/− mice

Metabolic consequences of reduced KGDHC activity have previously been investigated with ^{13}C labelled precursors using chemical inhibitors in cerebellar granule cells (Santos et al. 2006) and genetic manipulation of subunits in a kidney cell line (Shi et al. 2009). Both studies showed that glycolytic and GABA shunt activity were increased, the latter providing a way for metabolites to bypass the KGDHC step of the TCA cycle. Moreover, previous studies indicate that release of cytochrome c, caspase activation and biosynthetic pathways including that for the neurotransmitter acetylcholine are more sensitive to diminished KGDHC activity than measures of energy metabolism (Gibson and Blass 1976; Huang et al. 2003).

In the current study, reduced KGDHC activity caused a ~ 80 % increase in the concentration of glucose in the cortex, while the concentration of glucose in the cerebellum remained unchanged. The unaltered percentage [U-^{13}C]glucose in cortex shows that the concentration of [U-^{13}C]glucose increased in proportion to the total glucose concentration. Moreover, the total concentration of glucose and the percentage [U-^{13}C]glucose in serum of DLST +/− mice remained unaltered, showing that alterations in the brain were not due to peripheral changes in glucose metabolism. Furthermore, the fact that the concentration of glucose was unaltered in the cerebellum supports the idea that alterations in the delivery of glucose to the brain was not the cause of the change in the glucose concentration in cortex. The increased amount of glucose in cortex would point towards a reduced glycolysis, but no direct evidence of this was found, insofar as both the concentration and ^{13}C labelling of lactate, alanine, most amino acids (with the exception of aspartate) and the TCA cycle intermediates measured were unchanged. One possible explanation for this discrepancy is that the decrease in glucose utilization was caused by a compartment in which ^{13}C labelled acetyl CoA was used for energy production and not the labelling of amino acids.

The unaltered concentration of glutamate, level of [4,5-^{13}C]glutamate and percent M+2 glutamate show that decreased KGDHC activity did not alter glutamate metabolism. The only additional changes related to glucose metabolism in cortex were found in aspartate, in which both the total concentration and [1,2-^{13}C]aspartate and [3,4-^{13}C]aspartate were decreased. Both isotopomers are derived from OAA formed in the first turn of the TCA cycle rather than PC-mediated synthesis of OAA, because the latter would yield [1,2,3-^{13}C]aspartate. Aspartate aminotransferase (EC 2.6.1.1) is in approximately thermodynamic equilibrium in the rodent brain (Howse and Duffy 1975), so reductions in

aspartate were most likely a consequence of a decrease in the pool of OAA, in line with earlier findings (Santos et al. 2006). Selectively decreased aspartate levels have also been described in thiamine deficiency (TD) and partly attributed to decreased KGDHC activity (Navarro et al. 2008). Furthermore, two ratios estimating different aspects of metabolism were calculated for cortex, but no changes were found in PC versus PDHC activity or in ^{13}C enrichment of the acetyl CoA pool. The lack of change in PC versus PDHC activity in glutamate, glutamine and GABA formation supports that decreased KGDHC activity resulted in few changes in glucose metabolism in the compartments responsible for amino acid synthesis and degradation. In fact, the unaltered concentration of succinate and fumarate and percent of M+2 isotopomers of succinate, fumarate and malate indicates that labelled metabolites are somehow able to pass the KGDHC reaction. In addition, no ^{13}C labelled isotopomers derived from later turns of the TCA cycle were altered (results not shown), indicating that the ^{13}C label was able to stay in the TCA cycle for the same number of turns as in the controls, despite decreased KGDHC activity. However, no evidence of increased GABA shunt activity was found, in that the concentration and ^{13}C labelling of GABA and succinate remained unchanged. In summary, it appears that the KGDHC activity level in the DLST +/− mice is either sufficient to sustain TCA cycle metabolism, or that some compensatory mechanism has been established. It should, however, be noted that there is no compensatory upregulation of KGDH and DLD mRNA or protein level in DLST +/− mice (Yang et al. 2009).

All in all, results from cortex suggest that glucose and amino acid neurotransmitter metabolism is relatively well maintained during decreased KGDHC activity under physiological circumstances. However, in situations where the brain is metabolically challenged and the demand on ATP or neurotransmitters is increased, reduced KGDHC activity is likely a disadvantage that may accelerate or enhance mitochondrial dysfunction. It has already been shown that decreased KGDHC activity makes neurons more vulnerable to toxins and less able to cope with stress (Klivenyi et al. 2004; Yang et al. 2009). Furthermore, DLST +/− mice crossed with mice carrying the human amyloid precursor protein with two familial AD mutations (Tg19959) display accelerated amyloid pathology and earlier spatial learning and memory deficits compared to Tg19959 or DLST +/− mice alone (Dumont et al. 2009). Although few metabolic consequences of the possibly reduced glucose utilization in cortex were shown, the finding is exciting when it is related to the reduced glucose utilization commonly observed in AD. Our results suggest that a reduction in KGDHC activity has the ability to induce such a decrease in glucose utilization in the cortex and might therefore represent part of an early pathophysiological mechanism in AD.

In the cerebellum, no changes indicating altered glycolytic activity were found, as demonstrated by unaltered concentrations of glucose and alanine and ^{13}C labelling of lactate. Moreover, unaltered concentration of GABA and ^{13}C labelling of GABA and succinate indicated unaltered GABA shunt activity. In addition to the different methods of inducing decreased KGDHC activity, several experimental aspects could account for the different metabolic responses to reduced KGDHC activity in cerebellum *in vitro* (Santos et al. 2006) and in the current study. The *in vitro* experiment was performed on 1-week old cerebellar granule neurons, while the present experiment was performed in 6-weeks-old mice in which the cerebellum comprises additional types of neurons and also glia. Thus, our results largely represent the sum of metabolism in neurons and astrocytes, which might be of importance insofar as astrocytes appear more insensitive to reduction of KGDHC than neurons and have been shown to protect neurons during chronic impairment of oxidative metabolism (Park et al. 2000; Park et al. 2001). The time difference (1 versus 6 weeks) also allows time for compensatory mechanisms to be firmly established in the DLST +/− mice. Moreover, KGDHC in rats develops late compared to other TCA cycle enzymes. Given that regional KGDHC activity in mice follows the same developmental pattern, KGDHC activity

is different at age 1 and 6 weeks. Maximum activity level is reached on postnatal day 30 in both cerebral cortex and cerebellum, and is maintained during adulthood (Buerstatte et al. 2000). The activity in 10-day-old rats, however, is only 25–30 % of the maximum level. The difference in KGDHC activity during development has also been shown in whole brain homogenates from DLST +/− mice (Yang et al. 2009). Also, the rate of glucose oxidation through the TCA cycle during postnatal development is closely related to KGDHC activity (Buerstatte et al. 2000; Novotny et al. 2001). Consequently, initially different TCA cycle rate and KGDHC activity may give rise to differences in incorporation of ^{13}C label into metabolites or in responses to the activity reduction. It should also be noted that the high concentration of glucose used in the media used to culture the cells (> 25 mM) might have intensified the effect of decreased KGDHC activity since it has been shown that glucose loading exaggerates the effects of TD [see (Navarro et al. 2008) and references therein]. The results from the current study are thus not directly comparable to results from others (Santos et al. 2006), but contribute new insight into metabolic consequences of decreased KGDHC activity *in vivo*.

Cortex was more affected than cerebellum by the decrease in KGDHC activity. Several factors may contribute to this difference: initial KGDHC activity is higher in cortex than in the cerebellum (Lai and Cooper 1986), and *in situ* activity staining has shown that KGDHC activity decreases more in the cerebellum than in cortex as a response to heterozygote knockout of the DLST gene (Yang et al. 2009). In addition, the astrocyte-to-neuron ratio in cerebellum is lower and may make a difference in the impact of decreased KGDHC activity.

These results on DLST +/− mice complement rather exhaustive studies of thiamine deficiency (TD) [for review see (Karuppagounder and Gibson 2008)]. Thiamine is a co-factor for KGDHC, PDHC and transketolase. In rodents, PDHC is rather resistant to changes in thiamine availability (Butterworth et al. 1985; Butterworth et al. 1986; Gibson et al. 1984). Thus, TD produces deficits in KGDHC and transketolase. TD affects KGDHC activity to a different extent in different brain areas depending on the chosen method of induction (Butterworth et al. 1986), and the deficits in KGDHC induced by TD are only one to two weeks rather than through all development as the DLST +/− mice, so exact analogies are not possible. Nevertheless, some intriguing parallels do occur. Both TD (Zhao et al. 2008) and DLST +/− mice [the same as E2k +/− mice; (Calingasan et al. 2008)] have diminished neurogenesis, diminished *in vivo* glucose utilization (Hakim and Pappius 1981; Hakim and Pappius 1983), exaggerated plaque formation in plaque competent mice (Dumont et al. 2009; Karuppagounder et al. 2009), and decreased aspartate and OAA (Navarro et al. 2008). Together the data suggest that these common deficits in TD mice are due to the reduction in KGDHC and not to transketolase.

Taurine, NAA and tyrosine

Additional information regarding the status of brain cells can be obtained from metabolites that are not involved in glucose metabolism. Taurine is believed to exert a wide range of physiological effects in the brain [see (Huxtable 1992; Oja and Saransaari 1996) for reviews], and several studies also implicate that taurine protects against neuronal death during excitotoxicity (Chen et al. 2001; Louzada et al. 2004). Different mechanisms have been suggested, among others the ability of taurine to lower the concentration of intracellular cytoplasmic calcium during neuronal activation (Chen et al. 2001; El Idrissi and Trenkner 1999; Wu et al. 2005) and to activate $GABA_A$ receptors to counteract excessive glutamatergic neurotransmission (del Olmo et al. 2000; Louzada et al. 2004). Decreased level of taurine in the cerebrospinal fluid of patients with AD has also been reported (Csernansky et al. 1996; Pomara et al. 1992). Our results show that decreased KGDHC activity reduces the concentration of taurine in the cortex, possibly making cortical neurons more vulnerable to excitotoxic insult, which is implicated in neurodegeneration. However,

the lack of decrease in the NAA concentration in cortex indicates unaltered neuronal numbers or function at this age, supported by the fact that DLST +/− mice do not display neurodegenerative changes (Calingasan et al. 2008). NAA is synthesized in mitochondria (Madhavarao et al. 2003), is predominantly located in neurons (Moffett et al. 1991) and a decrease in NAA level is considered to reflect neuronal dysfunction or loss (Dautry et al. 2000; Demougeot et al. 2001; Valenzuela and Sachdev 2001). Moreover, the concentration of tyrosine, a precursor for the neurotransmitters dopamine, norepinephrine and epinephrine, was increased in the cerebellum. This in line with *in vitro* studies suggesting that neurotransmitter synthesis may be particularly sensitive to inhibition of KGDHC (Gibson and Blass 1976).

Conclusions

The results from this study show that a decrease in KGDHC activity reduced the glucose consumption in cortex, but did not have detrimental effects on mitochondrial metabolism in the brain insofar as only aspartate and thus probably OAA were decreased. Also, cortex was affected to a larger extent than the cerebellum. In situations in which the metabolic demand on cells may increase, reduced KGDHC activity most likely makes the brain more vulnerable and less able to cope with neuronal insults, and a decrease in glucose utilization might contribute to this. Future studies should be aimed at investigating the effects of the possible decrease in glucose utilization further, and the specific consequences in neurons and astrocytes should be studied in detail using simultaneous injection of ^{13}C labelled glucose and acetate combined with ^{13}C NMR spectroscopic analysis.

Acknowledgments

The authors thank Huan-Lian Chen for breeding and genotyping all of the mice, and Huan-Lian Chen and Saravanan Karuppagounder for their help with the injections of the mice and for help in the experimental design. The technical assistance of Anne B. Walls and Lars Evje is also gratefully acknowledged.

Grant number: The research was supported by NIH grant number PP-AG14930 and the Burke Medical Research Institute

References

Bak LK, Schousboe A, Sonnewald U, Waagepetersen HS. Glucose is necessary to maintain neurotransmitter homeostasis during synaptic activity in cultured glutamatergic neurons. J Cereb Blood Flow Metab. 2006; 26(10):1285–1297. [PubMed: 16467783]

Bergmeyer, HU.; Berndt, E.; Schmidt, F.; Stork, H. Glucose determination with hexokinase and glucose-6-phosphate dehydrogenase. In: Bergmeyer, HU., editor. Methods of Enzymatic Analysis. 2. New York: Academic Press; 1974. p. 1196-1201.

Bubber P, Haroutunian V, Fisch G, Blass JP, Gibson GE. Mitochondrial abnormalities in Alzheimer brain: mechanistic implications. Ann Neurol. 2005; 57(5):695–703. [PubMed: 15852400]

Buerstatte CR, Behar KL, Novotny EJ, Lai JC. Brain regional development of the activity of alpha-ketoglutarate dehydrogenase complex in the rat. Brain Res Dev Brain Res. 2000; 125(1–2):139–145.

Butterworth RF, Besnard AM. Thiamine-dependent enzyme changes in temporal cortex of patients with Alzheimer's disease. Metab Brain Dis. 1990; 5(4):179–184. [PubMed: 2087217]

Butterworth RF, Giguere JF, Besnard AM. Activities of thiamine-dependent enzymes in two experimental models of thiamine-deficiency encephalopathy: 1. The pyruvate dehydrogenase complex. Neurochem Res. 1985; 10(10):1417–1428. [PubMed: 4069311]

Butterworth RF, Giguere JF, Besnard AM. Activities of thiamine-dependent enzymes in two experimental models of thiamine-deficiency encephalopathy. 2. alpha-Ketoglutarate dehydrogenase. Neurochem Res. 1986; 11(4):567–577. [PubMed: 3724963]

Calingasan NY, Ho DJ, Wille EJ, Campagna MV, Ruan J, Dumont M, Yang L, Shi Q, Gibson GE, Beal MF. Influence of mitochondrial enzyme deficiency on adult neurogenesis in mouse models of neurodegenerative diseases. Neuroscience. 2008; 153(4):986–996. [PubMed: 18423880]

Chen WQ, Jin H, Nguyen M, Carr J, Lee YJ, Hsu CC, Faiman MD, Schloss JV, Wu JY. Role of taurine in regulation of intracellular calcium level and neuroprotective function in cultured neurons. J Neurosci Res. 2001; 66(4):612–619. [PubMed: 11746381]

Csernansky JG, Bardgett ME, Sheline YI, Morris JC, Olney JW. CSF excitatory amino acids and severity of illness in Alzheimer's disease. Neurology. 1996; 46(6):1715–1720. [PubMed: 8649576]

Dautry C, Vaufrey F, Brouillet E, Bizat N, Henry PG, Conde F, Bloch G, Hantraye P. Early N-acetylaspartate depletion is a marker of neuronal dysfunction in rats and primates chronically treated with the mitochondrial toxin 3-nitropropionic acid. J Cereb Blood Flow Metab. 2000; 20(5):789–799. [PubMed: 10826529]

del Olmo N, Bustamante J, del Rio RM, Solis JM. Taurine activates GABA(A) but not GABA(B) receptors in rat hippocampal CA1 area. Brain Res. 2000; 864(2):298–307. [PubMed: 10802037]

Demougeot C, Garnier P, Mossiat C, Bertrand N, Giroud M, Beley A, Marie C. N-Acetylaspartate, a marker of both cellular dysfunction and neuronal loss: its relevance to studies of acute brain injury. J Neurochem. 2001; 77(2):408–415. [PubMed: 11299303]

Dumont M, Ho DJ, Calingasan NY, Xu H, Gibson G, Beal MF. Mitochondrial dihydrolipoyl succinyltransferase deficiency accelerates amyloid pathology and memory deficit in a transgenic mouse model of amyloid deposition. Free Radic Biol Med. 2009; 47(7):1019–1027. [PubMed: 19596066]

El Idrissi A, Trenkner E. Growth factors and taurine protect against excitotoxicity by stabilizing calcium homeostasis and energy metabolism. J Neurosci. 1999; 19(21):9459–9468. [PubMed: 10531449]

Gibson GE, Blass JP. Inhibition of acetylcholine synthesis and of carbohydrate utilization by maple-syrup-urine disease metabolites. J Neurochem. 1976; 26(6):1073–1078. [PubMed: 945329]

Gibson GE, Haroutunian V, Zhang H, Park LC, Shi Q, Lesser M, Mohs RC, Sheu RK, Blass JP. Mitochondrial damage in Alzheimer's disease varies with apolipoprotein E genotype. Ann Neurol. 2000a; 48(3):297–303. [PubMed: 10976635]

Gibson GE, Ksiezak-Reding H, Sheu KF, Mykytyn V, Blass JP. Correlation of enzymatic, metabolic, and behavioral deficits in thiamin deficiency and its reversal. Neurochem Res. 1984; 9(6):803–814. [PubMed: 6149477]

Gibson GE, Park LC, Sheu KF, Blass JP, Calingasan NY. The alpha-ketoglutarate dehydrogenase complex in neurodegeneration. Neurochem Int. 2000b; 36(2):97–112. [PubMed: 10676873]

Gibson GE, Sheu KF, Blass JP, Baker A, Carlson KC, Harding B, Perrino P. Reduced activities of thiamine-dependent enzymes in the brains and peripheral tissues of patients with Alzheimer's disease. Arch Neurol. 1988; 45(8):836–840. [PubMed: 3395256]

Haberg A, Qu H, Haraldseth O, Unsgard G, Sonnewald U. In vivo injection of [1-13C]glucose and [1,2-13C]acetate combined with ex vivo 13C nuclear magnetic resonance spectroscopy: a novel approach to the study of middle cerebral artery occlusion in the rat. J Cereb Blood Flow Metab. 1998; 18(11):1223–1232. [PubMed: 9809511]

Hakim AM, Pappius HM. The effect of thiamine deficiency on local cerebral glucose utilization. Ann Neurol. 1981; 9(4):334–339. [PubMed: 7224598]

Hakim AM, Pappius HM. Sequence of metabolic, clinical, and histological events in experimental thiamine deficiency. Ann Neurol. 1983; 13(4):365–375. [PubMed: 6838172]

Hassel B, Bachelard H, Jones P, Fonnum F, Sonnewald U. Trafficking of amino acids between neurons and glia in vivo. Effects of inhibition of glial metabolism by fluoroacetate. J Cereb Blood Flow Metab. 1997; 17(11):1230–1238. [PubMed: 9390655]

Hassel B, Sonnewald U, Fonnum F. Glial-neuronal interactions as studied by cerebral metabolism of [2-13C]acetate and [1-13C]glucose: an ex vivo 13C NMR spectroscopic study. J Neurochem. 1995; 64(6):2773–2782. [PubMed: 7760058]

Howse DC, Duffy TE. Control of the redox state of the pyridine nucleotides in the rat cerebral cortex. Effect of electroshock-induced seizures. J Neurochem. 1975; 24(5):935–940. [PubMed: 167127]

Huang HM, Zhang H, Xu H, Gibson GE. Inhibition of the alpha-ketoglutarate dehydrogenase complex alters mitochondrial function and cellular calcium regulation. Biochim Biophys Acta. 2003; 1637(1):119–126. [PubMed: 12527416]

Huxtable RJ. Physiological actions of taurine. Physiol Rev. 1992; 72(1):101–163. [PubMed: 1731369]

Jones JG, Hansen J, Sherry AD, Malloy CR, Victor RG. Determination of acetyl-CoA enrichment in rat heart and skeletal muscle by 1H nuclear magnetic resonance analysis of glutamate in tissue extracts. Anal Biochem. 1997; 249(2):201–206. [PubMed: 9212871]

Karuppagounder, SS.; Gibson, GE. Thiamine deficiency: a model of metabolic encephalopathy and selective neuronal vulnerability. In: McCandless, DW., editor. Metabolic Encephalopathy. Springer Press; 2008. p. 235-260.

Karuppagounder SS, Xu H, Shi Q, Chen LH, Pedrini S, Pechman D, Baker H, Beal MF, Gandy SE, Gibson GE. Thiamine deficiency induces oxidative stress and exacerbates the plaque pathology in Alzheimer's mouse model. Neurobiol Aging. 2009; 30(10):1587–1600. [PubMed: 18406011]

Klivenyi P, Starkov AA, Calingasan NY, Gardian G, Browne SE, Yang L, Bubber P, Gibson GE, Patel MS, Beal MF. Mice deficient in dihydrolipoamide dehydrogenase show increased vulnerability to MPTP, malonate and 3-nitropropionic acid neurotoxicity. J Neurochem. 2004; 88(6):1352–1360. [PubMed: 15009635]

Lai JC, Cooper AJ. Brain alpha-ketoglutarate dehydrogenase complex: kinetic properties, regional distribution, and effects of inhibitors. J Neurochem. 1986; 47(5):1376–1386. [PubMed: 3760866]

Louzada PR, Lima ACP, Mendonca-Silva DL, Noël F, De Mello FG, Ferreira ST. Taurine prevents the neurotoxicity of beta-amyloid and glutamate receptor agonists: activation of GABA receptors and possible implications for Alzheimer's disease and other neurological disorders. The FASEB Journal. 2004; 18:511–518. [PubMed: 15003996]

Madhavarao CN, Chinopoulos C, Chandrasekaran K, Namboodiri MA. Characterization of the N-acetylaspartate biosynthetic enzyme from rat brain. J Neurochem. 2003; 86(4):824–835. [PubMed: 12887681]

Mastrogiacomo F, Bergeron C, Kish SJ. Brain alpha-ketoglutarate dehydrogenase complex activity in Alzheimer's disease. J Neurochem. 1993; 61(6):2007–2014. [PubMed: 8245957]

Melo TM, Nehlig A, Sonnewald U. Metabolism is normal in astrocytes in chronically epileptic rats: a (13)C NMR study of neuronal-glial interactions in a model of temporal lobe epilepsy. J Cereb Blood Flow Metab. 2005; 25(10):1254–1264. [PubMed: 15902201]

Melø TM, Sonnewald U, Bastholm IA, Nehlig A. Astrocytes may play a role in the etiology of absence epilepsy: A comparison between immature GAERS not yet expressing seizures and adults. Neurobiol Dis. 2007; 28(2):227–235. [PubMed: 17719229]

Moffett JR, Namboodiri MA, Cangro CB, Neale JH. Immunohistochemical localization of N-acetylaspartate in rat brain. Neuroreport. 1991; 2(3):131–134. [PubMed: 1768855]

Mosconi L, De Santi S, Li J, Tsui WH, Li Y, Boppana M, Laska E, Rusinek H, de Leon MJ. Hippocampal hypometabolism predicts cognitive decline from normal aging. Neurobiol Aging. 2008; 29(5):676–692. [PubMed: 17222480]

Navarro D, Zwingmann C, Butterworth RF. Region-selective alterations of glucose oxidation and amino acid synthesis in the thiamine-deficient rat brain: a re-evaluation using 1H/13C nuclear magnetic resonance spectroscopy. J Neurochem. 2008; 106(2):603–612. [PubMed: 18410518]

Nehlig A, Wittendorp-Rechenmann E, Lam CD. Selective uptake of [14C]2-deoxyglucose by neurons and astrocytes: high-resolution microautoradiographic imaging by cellular 14C-trajectography combined with immunohistochemistry. J Cereb Blood Flow Metab. 2004; 24(9):1004–1014. [PubMed: 15356421]

Norenberg MD. Distribution of glutamine synthetase in the rat central nervous system. J Histochem Cytochem. 1979; 27(3):756–762. [PubMed: 39099]

Norenberg MD, Martinez-Hernandez A. Fine structural localization of glutamine synthetase in astrocytes of rat brain. Brain Res. 1979; 161(2):303–310. [PubMed: 31966]

Novotny EJ Jr, Ariyan C, Mason GF, O'Reilly J, Haddad GG, Behar KL. Differential increase in cerebral cortical glucose oxidative metabolism during rat postnatal development is greater in vivo than in vitro. Brain Res. 2001; 888(2):193–202. [PubMed: 11150475]

Oja SS, Saransaari P. Taurine as osmoregulator and neuromodulator in the brain. Metab Brain Dis. 1996; 11(2):153–164. [PubMed: 8776717]

Park LC, Calingasan NY, Uchida K, Zhang H, Gibson GE. Metabolic impairment elicits brain cell type-selective changes in oxidative stress and cell death in culture. J Neurochem. 2000; 74(1):114–124. [PubMed: 10617112]

Park LC, Zhang H, Gibson GE. Co-culture with astrocytes or microglia protects metabolically impaired neurons. Mech Ageing Dev. 2001; 123(1):21–27. [PubMed: 11640948]

Pomara N, Singh R, Deptula D, Chou JC, Schwartz MB, LeWitt PA. Glutamate and other CSF amino acids in Alzheimer's disease. Am J Psychiatry. 1992; 149(2):251–254. [PubMed: 1734749]

Qu H, Haberg A, Haraldseth O, Unsgard G, Sonnewald U. (13)C MR spectroscopy study of lactate as substrate for rat brain. Dev Neurosci. 2000; 22(5–6):429–436. [PubMed: 11111159]

Reiman EM, Caselli RJ, Yun LS, Chen K, Bandy D, Minoshima S, Thibodeau SN, Osborne D. Preclinical evidence of Alzheimer's disease in persons homozygous for the epsilon 4 allele for apolipoprotein E. N Engl J Med. 1996; 334(12):752–758. [PubMed: 8592548]

Roberts E, Frankel S. gamma-Aminobutyric acid in brain: its formation from glutamic acid. J Biol Chem. 1950; 187(1):55–63. [PubMed: 14794689]

Saito K, Barber R, Wu J, Matsuda T, Roberts E, Vaughn JE. Immunohistochemical localization of glutamate decarboxylase in rat cerebellum. Proc Natl Acad Sci U S A. 1974; 71(2):269–273. [PubMed: 4131274]

Santos SS, Gibson GE, Cooper AJ, Denton TT, Thompson CM, Bunik VI, Alves PM, Sonnewald U. Inhibitors of the alpha-ketoglutarate dehydrogenase complex alter [1-13C]glucose and [U-13C]glutamate metabolism in cerebellar granule neurons. J Neurosci Res. 2006; 83(3):450–458. [PubMed: 16416424]

Shank RP, Bennett GS, Freytag SO, Campbell GL. Pyruvate carboxylase: an astrocyte-specific enzyme implicated in the replenishment of amino acid neurotransmitter pools. Brain Res. 1985; 329(1–2):364–367. [PubMed: 3884090]

Shi Q, Risa O, Sonnewald U, Gibson GE. Mild reduction in the activity of the alpha-ketoglutarate dehydrogenase complex elevates GABA shunt and glycolysis. J Neurochem. 2009; 109(Suppl 1): 214–221. [PubMed: 19393030]

Small GW, Mazziotta JC, Collins MT, Baxter LR, Phelps ME, Mandelkern MA, Kaplan A, La Rue A, Adamson CF, Chang L, et al. Apolipoprotein E type 4 allele and cerebral glucose metabolism in relatives at risk for familial Alzheimer disease. JAMA. 1995; 273(12):942–947. [PubMed: 7884953]

Taylor A, McLean M, Morris P, Bachelard H. Approaches to studies on neuronal/glial relationships by 13C-MRS analysis. Dev Neurosci. 1996; 18(5–6):434–442. [PubMed: 8940616]

Valenzuela MJ, Sachdev P. Magnetic resonance spectroscopy in AD. Neurology. 2001; 56(5):592–598. [PubMed: 11261442]

Wu H, Jin Y, Wei J, Jin H, Sha D, Wu JY. Mode of action of taurine as a neuroprotector. Brain Res. 2005; 1038(2):123–131. [PubMed: 15757628]

Waagepetersen HS, Qu H, Schousboe A, Sonnewald U. Elucidation of the quantitative significance of pyruvate carboxylation in cultured cerebellar neurons and astrocytes. J Neurosci Res. 2001; 66(5): 763–770. [PubMed: 11746400]

Yang L, Shi Q, Ho DJ, Starkov AA, Wille EJ, Xu H, Chen HL, Zhang S, Stack CM, Calingasan NY, Gibson GE, Beal MF. Mice deficient in dihydrolipoyl succinyl transferase show increased vulnerability to mitochondrial toxins. Neurobiol Dis. 2009; 36(2):320–330. [PubMed: 19660549]

Zhao N, Zhong C, Wang Y, Zhao Y, Gong N, Zhou G, Xu T, Hong Z. Impaired hippocampal neurogenesis is involved in cognitive dysfunction induced by thiamine deficiency at early pre-pathological lesion stage. Neurobiol Dis. 2008; 29(2):176–185. [PubMed: 17936635]

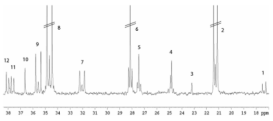

Figure 1.

Excerpt of a typical ^{13}C NMR spectrum of an extract from the cerebral cortex of a DLST +/− mouse injected with [U-^{13}C]glucose and decapitated 15 minutes later. Peak assignment: 1: Alanine C-3, 2: Lactate C-3, 3: NAA C6, 4: GABA C-3, 5: Glutamine C-3, 6: Glutamate C-3, 7: Glutamine C-4, 8: Glutamate C-4, 9: GABA C2, 10: Taurine C2, 11: Aspartate C-3, 12: Creatine C2. Parallel lines indicate that peaks are truncated.

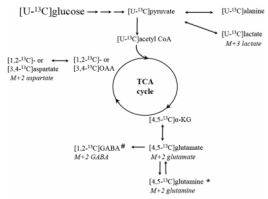

Figure 2.

A simplified schematic representation of some of the ^{13}C labelled isotopomers derived from cellular metabolism of [U-^{13}C]glucose. Via glycolysis, [U-^{13}C]glucose is converted to [U-^{13}C]pyruvate. The latter can be further converted to [U-^{13}C]alanine, lactate or acetyl Coenzyme A (acetyl CoA). When [U-^{13}C]acetyl CoA condenses with unlabelled oxaloacetate (OAA), [4,5-^{13}C]α-KG and subsequently [4,5-^{13}C]glutamate can be formed after several steps. This can further be converted to [4,5-^{13}C]glutamine in astrocytes or [1,2-^{13}C]GABA in GABAergic neurons. If the ^{13}C label stays in the TCA cycle, it can give rise to [1,2-^{13}C] or [3,4-^{13}C]OAA which is rapidly transaminated to aspartate labeled in the same position. The corresponding mass isotopomers detected with GC-MS are given under the positional isotopomers. * in astrocytes only, # in GABAergic neurons only.

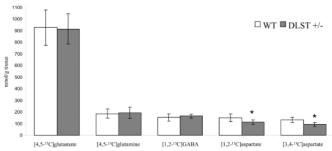

Figure 3.

Amounts (nmol/g tissue) of ^{13}C labelled metabolites derived from intermediates in the first turn of the TCA cycle in cerebral cortex extracts from wildtype (WT, white columns) and DLST +/− mice (gray columns). The mice were injected with [U-^{13}C]glucose (for details see Methods) and ^{13}C labelled metabolites were quantified using ^{13}C NMRS. Values are means ± standard deviation (n = 9 WT, n = 5 DLST +/−). Statistical analysis was performed using Student's *t*-test. * = $p < 0.05$, statistically significant difference between WT and DLST +/− mice.

Table I

Glucose, lactate and alanine concentrations and ^{13}C labelling in cortex, cerebellum and serum extracts from DLST +/− mice and wildtype mice (WT).

	Cortex		Cerebellum		Serum	
	WT	**DLST +/−**	**WT**	**DLST +/−**	**WT**	**DLST +/−**
Glucose						
mM	-	-	-	-	4.0 ± 0.3	4.5 ± 1.0 *a*
µmol/g	0.4 ± 0.2	0.8 ± 0.2 *b**	1.1 ± 0.3	1.5 ± 0.1 *b*	-	-
Percent [U-^{13}C]glucose	19.6 ± 5.6	15.8 ± 1.8 *c*	-	-	29.7 ± 4.8	30.5 ± 2.5 *a*
Lactate						
µmol/g *d*	6.9 ± 1.4	6.4 ± 1.2	-	-	-	-
Percent [U-^{13}C]lactate *e*	10.9 ± 1.4	9.8 ± 1.8	16.0 ± 2.5	16.0 ± 2.0	-	-
Alanine						
µmol/g	0.5 ± 0.1	0.6 ± 0.1 *d*	0.7 ± 0.2	1.0 ± 0.8 *f*	-	-
Percent [U-^{13}C]alanine *g*	12.1 ± 4.6	10.7 ± 2.2	-	-	-	-

Mice were injected with [U-^{13}C]glucose and decapitated 15 minutes later (for details see Materials and Methods). Values are means ± standard deviations. Statistical analysis was performed using Student's *t*-test.

a= quantified using ^{1}H NMRS (n = 4 WT, n = 4 DLST +/−)

b= quantified with glucose assay (n = 7 WT, n = 5 DLST +/− for cortex, n = 9 WT, n = 7 DLST +/− for cerebellum)

c= calculated from glucose assay values and ^{13}C NMRS (n = 7 WT, n = 4 DLST +/−)

d= quantified using ^{1}H NMRS (n = 9 WT, n = 6 DLST +/−)

e= measured by GC-MS (n = 9 WT, n = 6 DLST +/−)

f= quantified using HPLC (n = 9 WT, n = 7 DLST +/−)

g= calculated from ^{13}C NMR and ^{1}H NMRS (n = 9 WT, n = 5 DLST +/−).

*= $p < 0.05$, statistically significant difference between WT and DLST +/− mice.

Table II

Metabolite concentration in brain extracts from cortex and cerebellum (μmol/g tissue) of DLST +/−compared with wildtype mice (WT).

	Cortex (μmol/g) [a]		Cerebellum (μmol/g) [b]	
	WT	**DLST +/−**	**WT**	**DLST +/−**
Glutamate	6.90 ± 0.65	6.93 ± 0.45	9.31 ± 2.07	9.79 ± 2.56
Glutamine	2.32 ± 0.22	2.43 ± 0.68	6.11 ± 1.66	6.44 ± 2.12
GABA	1.93 ± 0.36	1.92 ± 0.37	2.04 ± 0.68	1.93 ± 0.48
Succinate	0.31 ± 0.13	0.38 ± 0.17	-	-
Fumarate	0.08 ± 0.02	0.09 ± 0.03	-	-
Aspartate	2.52 ± 0.41	1.78 ± 0.28*	3.59 ± 0.99	2.88 ± 0.71
Taurine	8.71 ± 0.76	7.65 ± 0.96*	7.65 ± 1.85	7.04 ± 1.56
Tyrosine	-	-	0.42 ± 0.17	0.61 ± 0.14*
NAA	4.50 ± 0.31	4.20 ± 0.70	-	-

Amounts of metabolites in cortex and cerebellum of DLST +/−compared with wildtype mice (WT). Values are means ± standard deviations. Statistical analysis was performed using Student's *t*-test.

[a] = quantified using ^{1}H NMRS (n = 9 WT, n = 6 DLST +/−)

[b] = quantified using HPLC (n = 9 WT, n = 7 DLST +/−)

* = $p < 0.05$, statistically significant difference between WT and DLST +/− mice.

Table III

Percentage metabolite with ^{13}C label in two positions of the molecule (M+2 isotopomers) in cortex and cerebellum of DLST +/− and wildtype mice (WT).

Metabolite with ^{13}C label in two carbon atoms	Cortex (%)		Cerebellum (%)	
	WT	DLST +/−	WT	DLST +/−
Glutamate	13.8 ± 1.7	13.6 ± 1.3	15.5 ± 2.0	16.1 ± 1.3
Glutamine	7.1 ± 1.0	6.9 ± 0.9	9.0 ± 1.7	9.6 ± 0.8
GABA	11.4 ± 1.3	11.4 ± 1.2	12.8 ± 1.3	13.6 ± 0.9
Succinate	6.9 ± 1.7	5.7 ± 0.9	3.8 ± 1.7	3.1 ± 2.0
Fumarate	4.7 ± 0.9	4.3 ± 1.1	10.8 ± 1.7	11.3 ± 1.0
Malate	6.3 ± 0.9	5.3 ± 1.0	11.2 ± 1.7	11.8 ± 1.1
Aspartate	8.3 ± 1.2	7.1 ± 1.1	10.2 ± 1.5	10.3 ± 0.9

Mice were injected with [U-^{13}C]glucose and decapitated 15 minutes later. Values are means ± standard deviation in percentage (n = 9 WT, n = 6 DLST +/−). The percentages were measured using GC-MS; for details see Materials and Methods. Statistical analysis was performed using Student's *t*-test with $p < 0.05$ regarded as significant.

Table IV

Metabolic ratios in the cortex of wildtype (WT) and DLST +/− mice

	Double/mono-labelled Glu C3		PC/PDHC activity	
	WT	DLST +/−	WT	DLST +/−
Glutamate	0.55 ± 0.12	0.43 ± 0.07	0.08 ± 0.01	0.08 ± 0.01
Glutamine	-	-	0.34 ± 0.08	0.43 ± 0.14
GABA	-	-	0.19 ± 0.04	0.19 ± 0.03

The ratio of double/mono-labelled glutamate C-3 represents the ^{13}C enrichment of the acetyl CoA pool entering the TCA cycle and the pyruvate carboxylation over pyruvate dehydrogenase (PC/PDHC) ratios for glutamate, glutamine and GABA in cortex of DLST +/− and wildtype (WT) mice. The ratios were calculated as described in Materials and Methods. Values are means ± standard deviation (n = 9 WT and n = 5 DLST +/−). Statistical analysis was performed using Student's *t*-test with $p < 0.05$ regarded as significant.